Oral and Maxillofacial Surgery (2020) 24:485–493
https://doi.org/10.1007/s10006-020-00862-7

ORIGINAL ARTICLE

Critical-sized mandibular defect reconstruction using human dental pulp stem cells in a xenograft model-clinical, radiological, and histological evaluation

Juan G. Gutiérrez-Quintero[1] · Juan Y. Durán Riveros[1] · Carlos A. Martínez Valbuena[2] · Sofía Pedraza Alonso[1] · JC Munévar[3] · SM Viafara-García[3,4,5,6]

Received: 2 November 2019 / Accepted: 4 June 2020 / Published online: 10 July 2020

Abstract

Purpose This research evaluated clinical, histological, and radiological osseous regeneration in a critical-sized bilateral cortico-medullary osseous defect in model rabbits from New Zealand after receiving a hydroxyapatite matrix and polylactic polyglycolic acid (HA/PLGA) implanted with human dental pulp stem cells (DPSCs).

Methods Eight New Zealand rabbits with bilateral mandibular critical-sized defects were performed where one side was treated with an HA/PLGA/DPSC matrix and the other side only with an HA/PLGA matrix for 4 weeks.

Results An osseointegration was clinically observed as well as a reduction of 70% of the surgical lumen on one side and a 35% on the other. Histologically, there was neo-bone formation in HA/PLGA/DPSC scaffold and angiogenesis. A bone radiodensity (RD) of 80% was radiologically observed achieving density levels similar to mandibular bone, while the treatment with HA/PLGA matrix achieves RD levels of 40% on its highest peaks.

Conclusions HA/PLGA/DPSC scaffold was an effective in vivo method for mandibular bone regeneration in critical-sized defects induced on rabbit models.

Keywords Bone regeneration · Mesenchymal stem cells · Xenograft · HA/PLGA scaffolds · Regenerative medicine

Introduction

Structural and functional reconstruction on critical-sized defects is an important subject in conditions as trauma, cancer, and infections [1]. However, clinical and biological restrictions as aggressive and extensive treatments, and complications associated with autogenous bone grafts including multiple required surgeries, potential morbidity, and the limited quantity of donor tissues could compromise the bone regeneration in craniomaxillofacial defects [2, 3].

Allogeneic or xenogeneic grafts are considered as optional treatments despite their inherent limitations including immunogenic responses, infection, and pathogen transmission risks [4, 5]. For these reasons, bone tissue engineering has emerged as a potential therapy wherein different biological strategies have been developed to promote the three-fundamental osteogenic, osteoinductive, and osteoconductive features [6]. One of the most studied osteogenic therapeutic strategies is the use of undifferentiated cells with high proliferative potential and the ability to regenerate different tissues. In fact, many niches of human stem cells in the postnatal stage have been revealed such as bone marrow, peripheral blood, brain, skin, dental pulp, and periodontal ligament [6, 7].

Human dental pulp stem cells (DPSCs) derived from the ectomesenchyme were first isolated by Gronthos et al. [8], describing certain advantages such as access and capacity of immune-modulation, which make them an attractive

✉ Juan G. Gutiérrez-Quintero
juan.gutierrez.quintero@gmail.com

1 Department of Oral and Maxillofacial Surgery, School of Dentistry, Universidad El Bosque, Bogotá, Colombia

2 School of Dentistry, Universidad El Bosque, Bogota, Colombia

3 Unit of Basic Oral Investigation, School of Dentistry, Universidad El Bosque, Bogotá, Colombia

4 Centro de Investigación e Innovación Biomédica (CIIB), Universidad de los Andes, Santiago, Chile

5 Laboratory of Tissue Engineering and Biofabrication, School of Medicine, Universidad de los Andes, Santiago, Chile

6 Cells for Cells, Santiago, Chile

alternative in regenerative medicine [9], showing biological properties of differentiation in multiple cell lineages in the craniofacial system as the mandibular bone. However, the bone repair is not only stem cells therapy for critical-sized defects, but also require bone substitutes or scaffolds to encourage osteoconduction [10].

Different biomaterials either of natural sources such as cellulose or synthetic ceramic sources as hydroxyapatite (HA) have been used as scaffolds in bone reconstruction at the clinical level, restoring function and form in defects unable to reach self-renewal known as critical-sized defects [10], especially in particular bones as the mandible and their biological and mechanical features. HA is a complex mineral structure very similar to human bone (Ca_5 (PO^4)$_3$ (OH), which develop bone particles with the same chemical components. HA combined with polymers such as polylactic-polyglycolic acid (PLGA) increases the capabilities, and properties of migration, adhesion, differentiation, and cell proliferation of the host in bone defects [11, 12]. Therefore, we suggest that the use of HA/PLGA or its combination along with DPSCs could increase the osteogenic, osteoinductive, and osteoconductive potential in mandibular critical-sized defects.

We aimed to analyze clinical, radiological, and histological parameters for bone regeneration in critical-sized defects, using scaffolds as HA, PLGA and human dental pulp stem cells in rabbit jaws, a xenograft model.

Methods

Isolation, characterization, and culture of DPSCs

Dental pulp was harvested from the healthy extracted teeth for orthodontic reasons of patients attended at postgraduate dental clinics in El Bosque University with the informed consent approved previously by the Committee of Ethics of the Institution. All procedures were conducted according to standard regulations. Once the pulp tissue was cut into small pieces, the tissue was placed in DMEM (Dulbecco's modified Eagle medium; Gibco BRL, Grand Island, NY, USA) supplemented with 10% fetal bovine serum (Hyclone, Logan, UT, USA) and 200 U/mL heparin (Sigma-Aldrich, St. Louis, MO, USA). Then, the tissue was enzymatically dissociated in a solution of 3 mg/mL collagenase and 4 mg/mL dispase (Sigma-Aldrich, St. Louis, MO, USA). After obtaining an average 1×10^7 cells, they were subjected to magnetic separation (Miltenyi Biotec, Germany) and CD105 antibody conjugated magnetic microbeads, following the manufacturer's instructions. The eluted and enriched fraction of CD105+ DPSCs was immunophenotyped by flow cytometry using antibodies panel against CD73, CD105, CD90, CD34, and CD45.

HA/PLGA scaffolds

HA and PLGA (50/50) solutions were mixed (3:1 *w*/*w* ratio) in 0.2% chloroform at 25 °C for 24 h (288,306, Sigma-Aldrich, St. Louis, MO, USA). Once mixed and dissolved, HA/PLGA solution was spread on cylindrical replica mold during 2 h at −20 °C and then lyophilized to allow the acetone solvent to evaporate for 24–48 h (Heto PowerDry LL3000, Thermo Fisher Scientific, Waltham, MA, USA). HA/PLGA scaffolds were then cut into small cylinders (~ 9 mm in diameter and ~ 2 mm in height) which fitted the area of the 24 wells and rinsed with 70% alcohol followed by exposed under UV light overnight. DPSCs (5×10^5, between passages 3 to 6) were seeded into the HA/PLGA scaffold and were maintained in DMEM culture medium supplemented with fetal bovine serum 10%, 100 U/mL penicillin, and 100 mg/mL streptomycin during 24 h at 37 °C prior implementation in the critical-sized bone defect of the animal model.

Animal surgical procedure

We studied eight adult male albino rabbits (New Zealand) of 3-months-old and 3-kg body weight which were born and raised in a proper animal facility. This research was approved by the Institutional Animal Care and Ethics Committee for Animal Experimentation of El Bosque University.

Bilateral critical-sized defect was performed in all animals under general anesthesia with ketamine 35 mg/kg/day hydrochloride and xylazine (2%) 0.1 mg/kg. Regions of the mandibular base were shaved and disinfected bilaterally. Incisions in both mandibular base sides of ~2 cm as long as layer dissection and periosteum elevation were performed. Afterwards, circular critical-size defects of ~ 10 mm in diameter and ~ 3 mm in height were created with a hard drill #702 operated by low-speed handpiece (EX 203 Set NSK, Japan) and continuous irrigation of sterile saline solution 0.9%. Each animal was simultaneously used in both groups:—HA/PLGA/DPSCs and HA/PLGA. The left and right mandibular sides were randomized. The tissues were repositioned and layer-sutured to the skin and finally rinsed with chlorhexidine 0.2%. After 30 days of the postoperative, the animals were euthanized using CO_2 at a regulated flow equating to 20% of the cage volume per minute (Euthanex, Allentown, PA, USA).

Clinical, radiological, and histological assessment

For clinical assessment, all groups were monitored daily for 30 days. Thus, the intake, palpable bone repair, inflammation, infection, hematoma, or any signs associated with local inflammatory reactions were assessed.

New bone formation was measured by digital radiography system with standardizing parameters (90° angle, X-ray cone distance 10 cm, and exposure settings of 0.06 s and 4 mA).

Skull and mandibular structures were measured weekly for 1 month.

The regeneration zone blocks were extracted from the surgical bed and immersed in formaldehyde at 10% for 7 days. Blocks were gradually dehydrated, decalcified, and embedded in epoxy resin 6 mm. Serial cuts (200 μm) were obtained using a microtome (Leica 2500E, Milan, Italy). Slides were stained with hematoxylin and eosin for qualitative histological evaluation by light microscopy.

RT-qPCR analysis

mRNA expression levels of Runt-related transcription factor 2 (Runx2), osteopontin (OPN), alkaline phosphatase (ALP), and collagen type I (COL1) were measured after 30 days of scaffold implantation to determinate osteoblastic stage differentiation in each mandibular side. Total RNA was obtained using method (Zymo Research, Irvine, CA, USA). The total amount of RNA was quantified using a NanoDrop (Thermo Scientific, Waltham, MA, USA). RT-qPCR was performed using 10 ng of total RNA and a KAPA SYBR FAST One-Step RT-qPCR Master Mix (Wilmington, MA, USA). Primers were designed using Primer3 and are listed in Table 1. The reaction mixture consisted of 5.2 μl of template [10 ng/μl], 7.5 μl of KAPA SYBRR FAST qPCR Master Mix [2x], 0.3 μl of KAPA RT Enzyme Mix [50×], and 0.6 μL of primers [10 μM], in a final reaction volume of 15 μL. The temperature profile used was as follows: 55 °C for 10 min, 1 cycle at 95 °C for 1 min, followed by 40 cycles of amplification at 95 °C for 10 s and 60 °C for 60 s. Melting curves were obtained by temperature increasing from 65 to 95 °C in increments of 0.5 °C. All experiments were run in triplicate, and expression levels were calculated from the qPCR results based on the 2-Ct method. For these calculations, GAPDH and bone defects no DPSCs-laden or only with scaffolds (PLGA/HA) were used as controls and to normalize the fold change for the determination of mRNA levels.

Table 1 RT-qPCR primer sequences

Gen name	Direction	Sequence (5′–3′)
Runx2	Fw	CATCTAATGACACCACCAGGC
	Rw	GCCTACAAAGGTGGGTTTGA
OPN	Fw	AGCCGTGGGAAGGACAGTTATG
	Rw	GGAGTTTCCATG AAGCCACAAAC
COL1	Fw	TCAAAGGCAATGCTCAAACA
	Rw	ACATCAAGACAAGAACGAGG TGA
GAPDH	Fw	GAAGGTCGGAGTCAACGG
	Rw	GGAAGATGGTGATGGGAT

Statistical analysis

Clinical variables between treatment were analyzed by Mann-Whitney *U*, while Wilcoxon test was used to compare before and after treatment. Chi-squared and Fisher's tests were performed to determinate the associations between radiographic and histological assessments. All p values ≤ 0.05 were considered statistically significant with the software SPSS 18 (IBM Corporation, Armonk, NY, USA).

Results

Isolation and characterization of DPSCs

DPSCs were expanded in vitro and characterized by flow cytometry at the third passage through the evaluation of the expression of the markers that define its phenotype as CD73, CD105, CD90, CD34, and CD45 (Fig. 1). In addition, the cells obtained after 5 days of incubation were fibroblast-like and non-refringent and had well-defined spherical nuclei (data not shown).

Characterization of the PLGA/HA and PLGA scaffolds

HA/PLGA synthesized by wet precipitation method macroscopically had a semirigid spongy consistency of heterogeneous porosity with a size of 1 mm in height and 8 mm in diameter. In the SEM, homogeneous distribution of HA and PLGA is observed (Figs. 1b and 2a). The SEM revealed interconnectivity between the deep and superficial surfaces of the matrices between 65 and 75%, and the pore size varies between 300 and 500 μm (Fig. 2c, d). Chemical analysis of HA revealed a Ca/P molar ratio of 1.55, which is compatible with natural calcium hydroxyapatites. The X-ray diffraction analysis confirmed that HA displayed the characteristic profile of pure hydroxyapatite with calcium, phosphate, and oxygen peaks and carbon peaks related to PLGA content. This information confirmed the correct concentrations, atomic weight, and compositions without contaminants of the matrices used in the study (Fig. 2e).

Previous reports in our group showed in vitro adhesion and a proliferant behavior of DPSCs seeded in scaffolds which indicated that DPSCs could survive and adhere on HA/PLGA (75/25), and therefore, this material is suitable as cylindrical scaffold [13].

Local inflammatory reactions and wound healing

Once surgical procedure was performed (Fig. 3), the postsurgical evaluation did not show apparent rejection signs and infection neither. Regards to food intake, it was normalized when the suture was removed on the eighth day while animal weight remained stable in all cases. In others words, the wound healing did not present any adverse event.

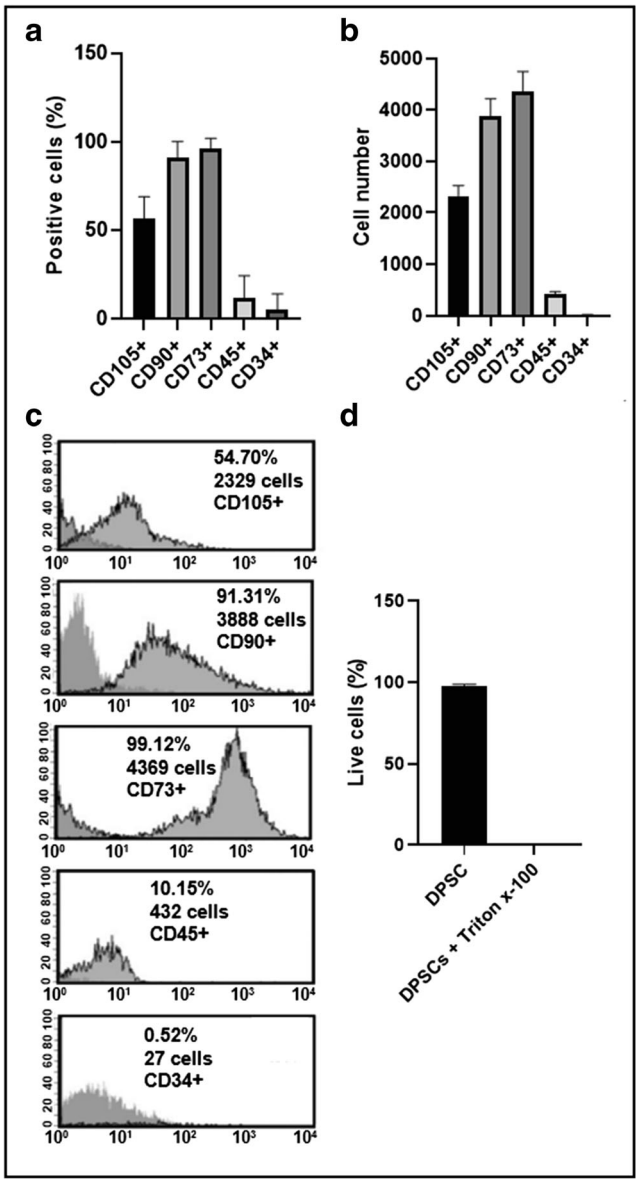

Fig. 1 Immunophenotyping of dental pulp stem cells (DPSCs) at passage 4 for the markers CD105, CD90, CD73, CD45, and CD34 and cell viability. **a** Positive DPSC (%) and **b** DPSC number expressing specific surface marker. **c** DPSC stained with antibodies against surface-specific markers (shaded profile) or an isotype-matched monoclonal antibody. This experiment is representative of the three performed. **d** DPSC viables (%) stained with Calcein AM to indicate intracellular esterase activity. All experiments were performed independently three times and analyzed by flow cytometer; the results are shown as the mean ± SEM ($n = 3$)

In vivo radiological findings

Taking into account that the jawbone is not completely radiopaque as the case of a restoration or metallic material, the percentage of radiodensity of 90% for the first radiographic time of the jawbone was taken without performing any treatment (Fig. 4a). During 4 weeks after surgical procedure, different in vivo X-rays showed increase in the radiodensity scale. After 1 and 2-week postsurgical, a statistically significant increase was found compared with the cell-free scaffold (Fig. 4b), obtaining a radiodensity percentage of 30% higher in the scaffold with cells ($P = 0.01$), considering it as onset of mineralization on experimental side (HA/PLGA/DPSCs). It was subsequently supported with the following radiographic times at third and fourth week postsurgical (Fig. 4c, d) due to an evident increase on the radiodensity scale between 70 and 80% in both radiographic times, thus obtaining a statistically significant difference during each week follow-up but mainly at the last week $P = 0.001$, while in the HA/PLGA side, the radiodensity scale increases up to 40% at fourth week postsurgical.

Ex vivo clinical evaluation

All scaffold edges showed osseointegration and bone callus formation at both treatments (Fig. 5). However, mandibular sides treated with HA/PLGA/DPSC obtained a greater decrease in the surgical bed area compared with HA/PLGA mandibular sides (Fig. 5a, b). Consequently, we evidenced a significant reduction in the bone defects for both treatments compared with the baseline or pretreatment ($P < 0.01$, Fig. 5c). In addition, we observed a significant difference between treatments, since HA/PLGA/DPSC mandibular sides showed the highest bone regeneration and lesion size reduction ($P < 0.05$, Fig. 5c).

Histological analysis

Despite both treatments encouraged osseointegration between scaffold and proximal host bone, animal mandibular sides treated with HA/PLGA/DPSC compared with HA/PLGA reached a differential bone regeneration, showing mainly more mature cancellous bone than lamellar bone on the sides treated with HA/PLGA/DPSC scaffolds ($P = 0.001$) (Fig. 6). Moreover, test group showed a significant cell presence of bone lineage and neovascular formation in regeneration areas on the sides treated with HA/PLGA/DPSC scaffolds compared with HA/PLGA scaffolds ($P = 0.002$) (Fig. 6a, b). Cartilaginous tissue formation or calcification process was not observed surrounding soft tissues.

Effect of HA/PLGA and HA/PLGA/DPSC scaffolds on osteogenic marker expression

HA/PLGA/DPSC scaffolds increased the expression of Runx2 mRNA (3-fold) relative to housekeeping gene and stronger transcriptional activation of ALP mRNA (11-fold), COL1 mRNA (20-fold), and OPN mRNA (76-fold), showing differential osteogenic expression between treatments ($P < 0.05$, Fig. 7).

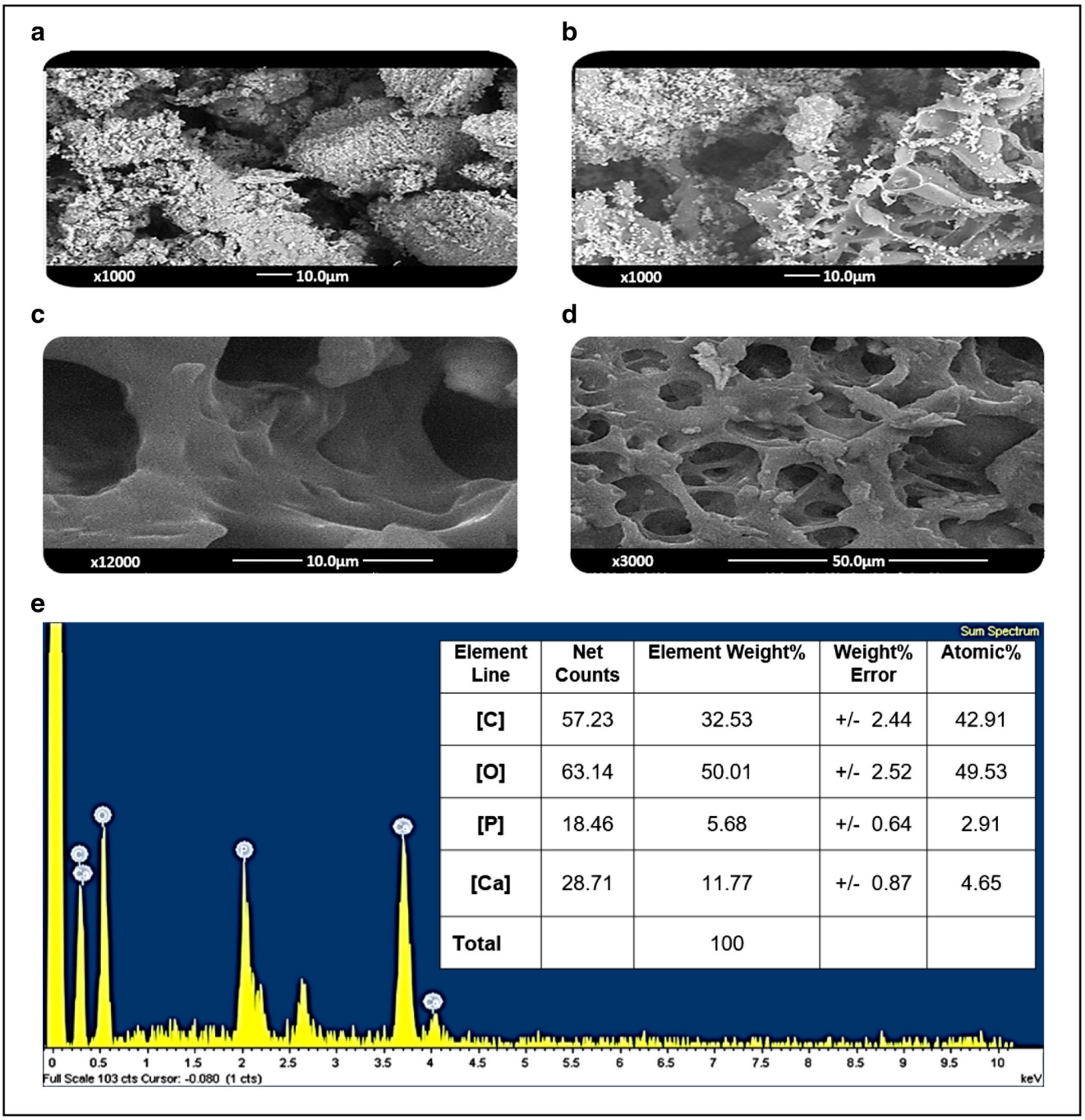

Fig. 2 Characterization of scaffolds. **a–d** SEM micrographs of PLGA/HA showing homogeneous distribution of the HA/PLGA and interconnectivity of 70% among the pores. **e** EDX scan spectra of PLGA/HA

Discussion

Critical-sized bone defect restoration is a major problem for oral and maxillofacial surgeons that impact patient's life quality. Different strategies and in vivo models have been based on autografts, allografts, and xenografts that provide properties such as osteoconduction, osteogenesis, and osteoinduction [10]. However, the use of stem cells on scaffolds has significantly improved and accelerated the bone healing [6].

The major sources of human mesenchymal stem cells can be distinguished between adult tissues, preferably bone marrow, peripheral blood and adipose tissue, and neonatal birth-associated tissues [14]. However, the technical difficulty for collection and strict conditions for donor patients have

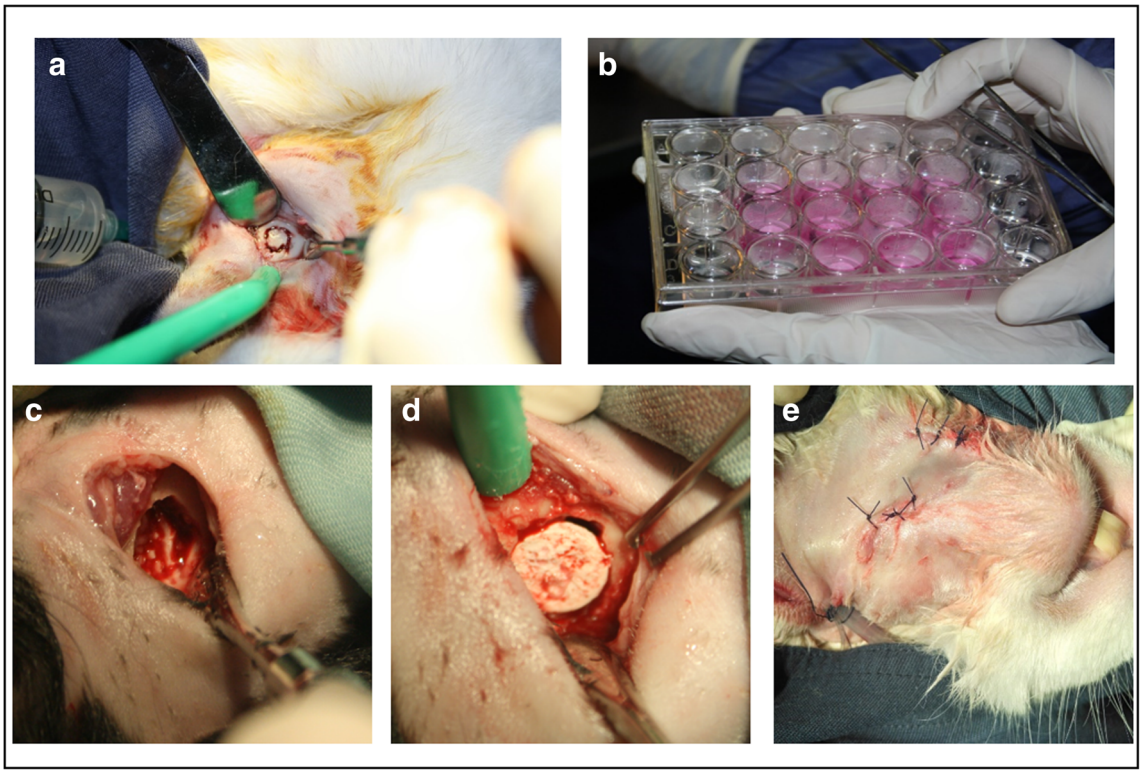

Fig. 3 Surgical procedure. **a** The mandibular periosteum was elevated. **b** Scaffold HA/PLGA or HA/PLGA before its placement. **c** A circle bone segment (3-cm defect) was removed. **d** Placement of scaffold HA/PLGA or HA/PLGA/DPSC in the surgical. **e** Suture by layers with silk 4-0

encouraged the exploration of alternative hMSC sources. Although the cell culture condition may affect the properties of stem cells [15, 16], DPSCs are reported to maintain an undifferentiated state even upon long-term cultivation [17], and to be influenced little by the number of passages [18], similar results previously reported in our group [13]. In addition, DPSCc offers some advantages over other human stem cells like accessibility, availability, and the multipotency, turning them into a better source for autologous, allogeneic, and xenogeneic clinical applications [8, 19].

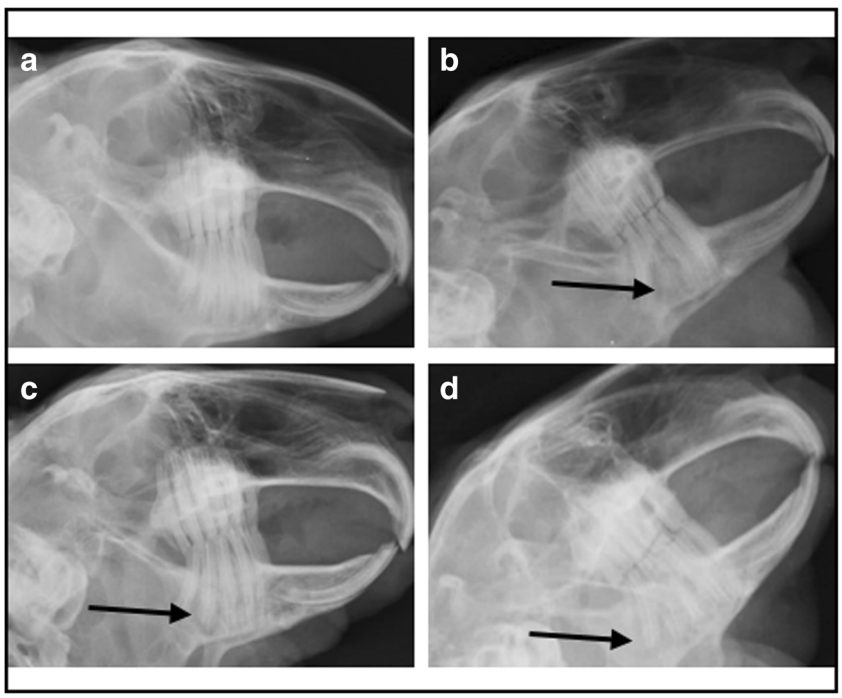

Fig. 4 X-ray radiographs of rabbit mandibular defects. **a** The X-rays at presurgical, **b** immediately postsurgical, **c** at second, and **d** fourth week postoperatively showed healing according to opacity density

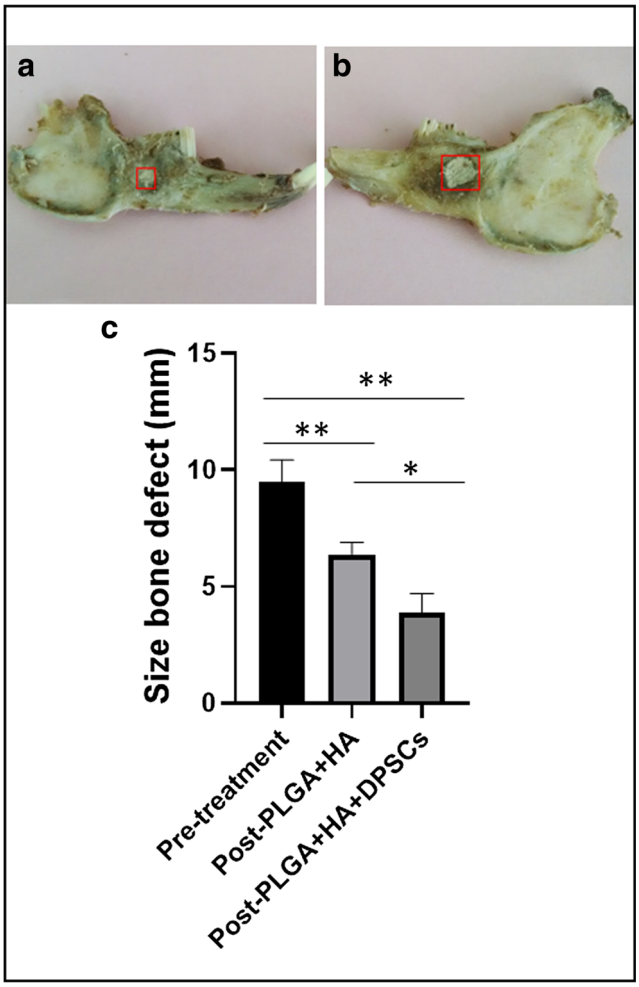

Fig. 5 Ex vivo clinical evaluation. **a** HA/PLGA/DPSC showed greater diameter reduction of the surgical bed and a transition between immature bone neoformation and mature bone neoformation compared with **b** HA/PLGA see red lines. Pretreatment and posttreatment with HA/PLGA/DPSC reached a $*P < 0.05$, $**P < 0.001$ (Wilcoxon test) while comparative posttreatment between HA/PLGA and HA/PLGA/DPSC reached a $*P < 0.05$ (Mann-Whitney *U*). **c**. Data are presented as the mean ± standard error of the mean of all critical-sized defects ($n = 8$)

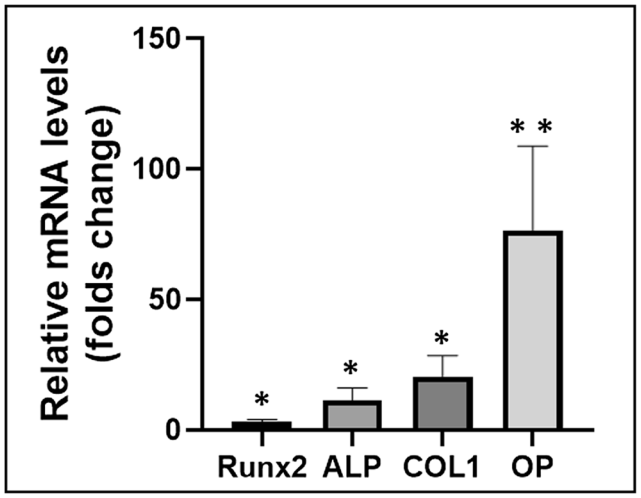

Fig. 7 Osteogenic marker analysis**.** Reverse transcription-quantitative polymerase chain reaction was performed to determine the mRNA expression levels of ALP, Runx2, OPN, and COL1 from mandibular sides treated with HA/PLGA/DPSCs. mRNA from mandibular sides treated with HA/PLGA was used only as controls. Data are presented as the mean ± standard error of the mean ($n = 3$). $*P < 0.05$ and $**P < 0.001$, as indicated using Wilcoxon test to compare intragroups. ALP alkaline phosphatase, Runx2 runt-related transcription factor 2, OPN osteopontin, COL1 collagen type 1, DPSCs dental pulp stem cells

In our study, critical-sized defects in rabbits treated with HA/PLGA scaffolds showed noticeable signs of repair in the fourth postoperative week. However, HA/PLGA/DPSC scaffolds showed better repairing signs, matching with the radiological repairing according to the radiodensity increasing scale, mainly during the last three postoperative weeks so it can be deduced that in scaffolds with cells, there is a better bone regeneration and even in a shorter time compared with matrices without DPSCs. Similar results have been described hard tissue regeneration using DPSCs in osteogenic scaffolds based on HA, highlighting the quality and significant presence of osteogenic cells also described in our study [20–24].

Although HA/PLGA scaffolds without DPSCs also offer bone regeneration, molecularly we found significant differences in mRNA levels of key osteogenic markers capable to determinate osteoblastic stage differentiation, skeletogenesis, and extracellular matrix secretion as Runx2, OPN, COL1, and ALP [25–28], especially after treating critical-sized defects with HA/PLGA/DPSCs. Therefore, it could explain the highest percent of bone regeneration (70–80%) reached in

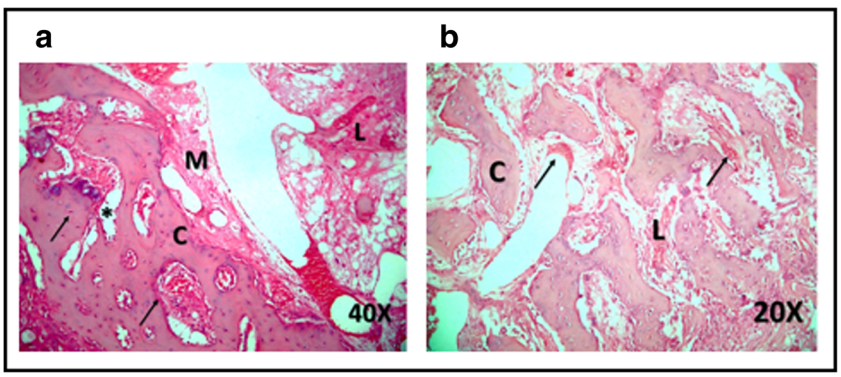

Fig. 6 H&E staining. **a** HA/PLGA/DPSCs and **b** HA/PLGA staining after 30 days of implantation. M: HA/PLGA/DPSC scaffold. L lamellar bone, C cancellous bone. Arrow: neovascularization. I intermediate zone. Asterisk indicates medullary space

our study. However, other factors or cytokines could take place in our in vivo bone regeneration approach such as bone morphogenetic protein (BMP), a key osteogenic and osteoinducer growth factor that encourages bone formation through the recruitment and differentiation of adjacent tissue stem cells in bone lineage [21, 29]. Further researches are also required to assess if the DPSCs or their soluble factors are involved in bone regeneration compared with the autogenic stem cell response. Besides, other parameters could be considered in our future studies such as biomechanical properties of the bone formed, mandibular function, microarchitecture bone quality, and the comparative response between HA/PLGA/DPSCs and HA/PLGA/BM-MSCs (bone marrow-mesenchymal stem cells).

Conclusions

HA/PLGA scaffolds provide osteoconductive properties, and DPSCs seem to provide osteogenic properties showing significant results in bone regeneration compared with HA/PLGA scaffold after 4 weeks. However, it is necessary to perform further preclinical and clinical studies that not only involve longer term but also the role of other factors as immune response, host immunomodulation, and the role of secretome, exosome, and soluble factors are not clearly understood during the bone regeneration.

Funding information This study was funded by a COLCIENCIAS 61702013 National Grant and a PCI 2012-342 Universidad El Bosque Grant.

Compliance with ethical standards

Conflict of interest The authors declare that they have no conflict of interest.

Ethical approval All applicable international, national, and institutional guidelines for the care and use of animals were followed.

References

1. Marei HF, Mahmood K, Almas K (2018) Critical size defects for bone regeneration experiments in the dog mandible: a systematic review. Implant Dent 27(1):135–141
2. Brierly G, Tredinnick S, Lynham A, Woodruff M (2016) Critical sized mandibular defect regeneration in preclinical in vivo models. Curr Mol Biol Rep 2(2):83–89
3. Kim DH, Rhim R, Li L, Martha J, Swaim BH, Banco RJ, Jenis LG, Tromanhauser SG (2009) Prospective study of iliac crest bone graft harvest site pain and morbidity. Spine J 9(11):886–892
4. Wiltfang J, Zernial O, Behrens E, Schlegel A, Warnke PH, Becker ST (2012) Regenerative treatment of peri-implantitis bone defects with a combination of autologous bone and a demineralized xenogenic bone graft: a series of 36 defects. Clin Implant Dent Relat Res 14(3):421–427
5. Yildirim M, Spiekermann H, Biesterfeld S, Edelhoff D (2000) Maxillary sinus augmentation using xenogenic bone substitute material Bio-Oss in combination with venous blood. A histologic and histomorphometric study in humans. Clin Oral Implants Res 11(3): 217–229
6. Dang M, Saunders L, Niu X, Fan Y, Ma PX (2018) Biomimetic delivery of signals for bone tissue engineering. Bone Res 6(1):1–12
7. Aloise AC, Pelegrine AA, Zimmermann A, de Mello E, Oliveira R, Ferreira LM (2015) Repair of critical-size bone defects using bone marrow stem cells or autogenous bone with or without collagen membrane: a histomorphometric study in rabbit calvaria. Int J Oral Maxillofac Implants 30(1):208–215
8. Gronthos S, Mankani M, Brahim J, Robey PG, Shi S (2000) Postnatal human dental pulp stem cells (DPSCs) in vitro and in vivo. Proc Natl Acad Sci U S A 97(25):13625–13630
9. Zhang Y, Xing Y, Jia L, Ji Y, Zhao B, Wen Y et al (2018) An in vitro comparative study of multi-sources derived mesenchymal stem cells for bone tissue engineering. Stem Cells Dev 27(23): 1634–1645
10. Billström GH, Blom AW, Larsson S, Beswick AD (2013) Application of scaffolds for bone regeneration strategies: current trends and future directions. Injury 44(Suppl 1):28
11. Dinarvand P, Seyedjafari E, Shafiee A, Jandaghi AB, Doostmohammadi A, Fathi MH et al (2011) New approach to bone tissue engineering: simultaneous application of hydroxyapatite and bioactive glass coated on a poly(L-lactic acid) scaffold. ACS Appl Mater Interfaces 3(11):4518–4524
12. Zong C, Qian X, Tang Z, Hu Q, Chen J, Gao C, Tang R, Tong X, Wang J (2014) Biocompatibility and bone-repairing effects: comparison between porous poly-lactic-co-glycolic acid and nano-hydroxyapatite/poly(lactic acid) scaffolds. J Biomed Nanotechnol 10(6):1091–1104
13. Jiménez NT, Carlos Munévar J, González JM, Infante C, Lara SJP (2018) In vitro response of dental pulp stem cells in 3D scaffolds: a regenerative bone material. Heliyon 4(9):e00775
14. Hass R, Kasper C, Böhm S, Jacobs R (2011) Different populations and sources of human mesenchymal stem cells (MSC): a comparison of adult and neonatal tissue-derived MSC. Cell Commun Signal 9:12
15. Kawashima N, Noda S, Yamamoto M, Okiji T (2017) Properties of dental pulp–derived mesenchymal stem cells and the effects of culture conditions. J Endod 43:S31–S34
16. Sotiropoulou PA, Perez SA, Salagianni M, Baxevanis CN, Papamichail M (2006) Characterization of the optimal culture conditions for clinical scale production of human mesenchymal stem cells. Stem Cells 24:462–471
17. Suchánek J, Soukup T, Ivancaková R, Karbanová J, Hubková V, Pytlík R, Kucerová L (2007) Human dental pulp stem cells–isolation and long term cultivation. Acta Medica (Hradec Kralove) 50(3):195–201
18. Lizier NF, Kerkis A, Gomes CM, Hebling J, Oliveira CF, Caplan AI, Kerkis I (2012) Scaling-up of dental pulp stem cells isolated from multiple niches. PLoS One 7:e39885. https://doi.org/10.1371/journal.pone.0039885
19. Scadden DT (2006) The stem-cell niche as an entity of action. Nature 441(7097):1075–1079
20. Ragetly GR, Griffon DJ (2011) The rationale behind novel bone grafting techniques in small animals. Vet Comp Orthop Traumatol 24(1):1–8
21. Akkouch A, Zhang Z, Rouabhia M (2014) Engineering bone tissue using human dental pulp stem cells and an osteogenic collagen-hydroxyapatite-poly (L-lactide-co-ε-caprolactone) scaffold. J Biomater Appl 28(6):922–936
22. D'Antò V, Raucci MG, Guarino V, Martina S, Valletta R, Ambrosio L (2016) Behaviour of human mesenchymal stem cells

on chemically synthesized HA-PCL scaffolds for hard tissue regeneration. J Tissue Eng Regen Med 10(2):147
23. Zheng L, Yang F, Shen H, Hu X, Mochizuki C, Sato M, Wang S, Zhang Y (2011) The effect of composition of calcium phosphate composite scaffolds on the formation of tooth tissue from human dental pulp stem cells. Biomaterials 32(29):7053–7059
24. Abu-Serriah MM, Odell E, Lock C, Gillar A, Ayoub AF, Fleming RH (2004) Histological assessment of bioengineered new bone in repairing osteoperiosteal mandibular defects in sheep using recombinant human bone morphogenetic protein-7. Br J Oral Maxillofac Surg 42(5):410–418
25. Komori T (2010) Regulation of bone development and extracellular matrix protein genes by RUNX2. Cell Tissue Res 339(1):189–195
26. Izu Y, Ezura Y, Koch M, Birk DE, Noda M (2016) Collagens VI and XII form complexes mediating osteoblast interactions during osteogenesis. Cell Tissue Res 364(3):623–635
27. Poundarik AA, Boskey A, Gundberg C, Vashishth D (2018) Biomolecular regulation, composition and nanoarchitecture of bone mineral. Sci Rep 8(1):1191
28. Wennberg C, Hessle L, Lundberg P, Mauro S, Narisawa S, Lerner UH, Millán JL (2000) Functional characterization of osteoblasts and osteoclasts from alkaline phosphatase knockout mice. J Bone Miner Res 15(10):1879–1888
29. Vahabi S, Amirizadeh N, Shokrgozar MA, Mofeed R, Mashhadi A, Aghaloo M, Sharifi D, Jabbareh L (2012) A comparison between the efficacy of Bio-Oss, hydroxyapatite tricalcium phosphate and combination of mesenchymal stem cells in inducing bone regeneration. Chang Gung Med J 35(1):28–37